Effects of MWNT nanofillers on structures and properties of PVA electrospun nanofibres

2007 Nanotechnology 18 225605

(http://iopscience.iop.org/0957-4484/18/22/225605)

Nanotechnology **18** (2007) 225605 (8pp) doi:10.1088/0957-4484/18/22/225605

Effects of MWNT nanofillers on structures and properties of PVA electrospun nanofibres

Minoo Naebe[1], Tong Lin[1,4], Wendy Tian[2], Liming Dai[3] and Xungai Wang[1]

[1] Centre for Material and Fibre Innovation, Deakin University, Geelong, VIC 3217, Australia
[2] Molecular and Health Technologies, Commonwealth Scientific and Industrial Research Organisation, Clayton, VIC 3169, Australia
[3] Department of Chemical and Materials Engineering, The University of Dayton, Dayton, OH 45469, USA

E-mail: tong.lin@deakin.edu.au

Received 25 January 2007, in final form 21 March 2007
Published 4 May 2007
Online at stacks.iop.org/Nano/18/225605

Abstract
In this study, we have electrospun poly(vinyl alcohol)(PVA) nanofibres and PVA composite nanofibres containing multi-wall carbon nanotubes (MWNTs) (4.5 wt%), and examined the effect of the carbon nanotubes and the PVA morphology change induced by post-spinning treatments on the tensile properties, surface hydrophilicity and thermal stability of the nanofibres. Through differential scanning calorimetry (DSC) and wide-angle x-ray diffraction (WAXD) characterizations, we have observed that the presence of the carbon nanotubes nucleated crystallization of PVA in the MWNTs/PVA composite nanofibres, and hence considerably improved the fibre tensile strength. Also, the presence of carbon nanotubes in PVA reduced the fibre diameter and the surface hydrophilicity of the nanofibre mat. The MWNTs/PVA composite nanofibres and the neat PVA nanofibres responded differently to post-spinning treatments, such as soaking in methanol and crosslinking with glutaric dialdehyde, with the purpose of increasing PVA crystallinity and establishing a crosslinked PVA network, respectively. The presence of carbon nanotubes reduced the PVA crystallization rate during the methanol treatment, but prevented the decrease of crystallinity induced by the crosslinking reaction. In comparison with the crosslinking reaction, the methanol treatment resulted in better improvement in the fibre tensile strength and less reduction in the tensile strain. In addition, the presence of carbon nanotubes reduced the onset decomposition temperature of the composite nanofibres, but stabilized the thermal degradation for the post-spinning treated nanofibres. The MWNTs/PVA composite nanofibres treated by both methanol and crosslinking reaction gave the largest improvement in the fibre tensile strength, water contact angle and thermal stability.

(Some figures in this article are in colour only in the electronic version)

1. Introduction

Carbon nanotubes (CNTs) with a high aspect ratio and low density have been shown to possess excellent mechanical, thermal and electronic properties [1]. These characteristics make them an ideal candidate as a filler to develop potentially revolutionary composites with light weight and enhanced mechanical [2, 3], electrical [4, 5] or thermal properties [6, 7]. Polymer fibres reinforced with CNTs are of particular interest. [3, 8–15]. Super-tough CNT composite fibres have

[4] Author to whom any correspondence should be addressed.

been produced by spinning single-wall carbon nanotubes (SWNTs) into poly(vinyl alcohol)(PVA) solution [3, 8, 9]. The mechanical properties of the composite fibres are highly dependent on the dispersion and the microscopic orientation of carbon nanotubes in the polymer matrix, and their interfacial interactions with the polymer.

Recently, electrospinning has been used to produce ultra-fine CNT composite fibres. The electrospinning process involves stretching a polymer solution under a strong electric field to form dry or semi-dry fibres with diameters on the nanometre scale [16–19]. From solution to dry fibre, the fibre stretching process takes just tens of milliseconds [20]. With such a fast fibre-stretching speed and high aspect ratio of the resultant nanofibre, an alignment of CNTs along the axis of the nanofibre could be achieved when a polymer solution containing well-dispersed carbon nanotubes is electrospun [14, 15, 21, 22]. The electrospun nanofibres can be collected in the form of a randomly oriented non-woven mat, aligned nanofibre array and continuous nanofibre yarn, which have shown enormous potential in diverse applications.

Electrospun composite fibres of MWNTs with different polymers such as polyethylene oxide (PEO) [15, 23], polyacrylonitrile (PAN) [24, 25], polyvinyl alcohol(PVA) [23], polycarbonate (PC) [26], nylon [27], polymethyl methacrylate (PMMA) [28] and poly(vinyl acetate) (PVAc) [29] have been reported. These composite nanofibres have shown enhanced fibre mechanical properties and improved electrical conductivity also. However, systematic study on the carbon nanotube–matrix interaction has been scarce in the research literature.

PVA is a semi-crystal hydrophilic polymer consisting of one hydroxyl group in each repeat unit and hence crosslinkable. The carbon nanotube/PVA composite film and fibre have received a great deal of attention because of their excellent mechanical properties and combined electrical/thermal conductivity unavailable in other composite materials [3, 8, 30, 31]. Recent research [2, 30–38] has indicated that CNTs nucleate crystallization of PVA, and a crystalline PVA layer formed around the nanotubes accounts for the excellent mechanical properties of the composite materials.

PVA is also one of the major polymer systems being studied in the electrospinning field. The electrospinnability of PVA is affected by electrospinning parameters [17], the PVA molecular weights [39, 40] and hydrolyzed degrees [41], solution pH values [42] and additives [43, 44]. The PVA nanofibres have been used as drug carriers for controlled release [45, 46]. Although electrospun CNTs/PVA nanofibres have been reported [23], it has not been established if the nucleation crystallization of PVA occurs within the electrospun composite CNTs/PVA fibres, and if the fast fibre stretching in electrospinning would obstruct this nucleation crystallization process.

It has been well established that the polymer morphology, the overall form of polymer structure, is an important factor in determining the material properties. The change of PVA crystallinity and the formation of a crosslinked PVA network achieved by a post-spinning treatment have been found to improve fibre mechanical properties [43, 47]. It has not yet been established if the mechanical properties of a composite CNTs/PVA fibre can be improved through the change of PVA morphology induced by a post-treatment.

In this study, we used multi-wall carbon nanotubes (MWNTs)/PVA composite nanofibres as a model material to examine the effects of carbon nanotubes and the PVA morphological changes on the polymer crystallinity, tensile properties, surface hydrophility and thermal stability of the composite fibres. Possible effects of the post-spinning treatments by soaking in methanol, crosslinking with glutaric dialdehyde, or both, are also discussed. This study will contribute to the understanding of the role of polymer matrix and filler–matrix interaction in improving the properties of CNTs/polymer composite fibres. In addition, the MWNTs/PVA nanofibres may find applications in biomedical areas, as drug carriers for controlled release for instance.

2. Experimental details

2.1. Materials and measurements

PVA (average molecular weight = 146 000–186 000, 96% hydrolyzed) and all other chemicals were obtained from Aldrich-Sigma and used as received. The MWNTs were provided by CSIRO and were purified by refluxing in 3N HNO_3 for 48 h prior to use.

The electrospun nanofibres were observed under a scanning electron microscope (SEM Leica S440) and a transmission electron microscope (TEM, Model 2000 FE, Hitachi Corp). The fibre diameter was calculated based on the SEM images with the aid of a software package (Image *Pro Plus 4.5*). The mechanical properties of the nanofibre mats were measured with a universal tensile tester (Lloyd), according to ASTM D-882. Differential scanning calorimetry (DSC) was performed using DSC 821 (Mettler Toledo). A specimen of approximately 5 mg was encapsulated in an aluminium pan (13 mg) and measured in alternating DSC mode at an underlying heating rate of 10 °C min^{-1}. Before the DSC measurements, the samples were vacuum dried for 72 h at room temperature in the presence of phosphorus pentoxide. Wide-angle x-ray diffraction (WAXD) was done on a powder diffractometer (Philips 1140/90) with Cu radiation 1.5406 Å. Fourier transform infrared (FTIR) spectra were recorded by a FTIR spectrophotometer (Bruker optics), using the KBr method. The water contact angles were measured using a contact angle meter (KSV CAM200 Instruments Ltd). Thermo-gravimetric analysis (TGA) was performed with a Mettler Toledo TGA/STDA851. The specimens were placed in a ceramic pan and tested in air flow at a heating rate of 10 °C min^{-1}.

2.2. Electrospinning of MWNTs/PVA nanofibres

PVA aqueous solution (16 wt%) was prepared by dissolving PVA powder in distilled water at 90 °C with constant stirring for about 12 h. A mixture of the purified MWNTs (245 mg) and water (6.25 ml) was ultrasonicated for about 5 h and then mixed with the PVA solution (16 wt%, 33.75 ml). During the ultrasonic process, the solution was cooled in an ice/water bath to avoid solution overheating. The solution was further ultrasonicated for 1 h to obtain homogeneous dispersion. The

Table 1. Fibre diameters, tensile properties and water contact angles.

	Pure PVA nanofibre mats				MWNTs/PVA nanofibre mats			
	Diameter (nm)	Tensile strength (MPa)	Strain (%)	Contact angle	Diameter (nm)	Tensile strength (MPa)	Strain (%)	Contact angle
Non-treatment	684 ± 220	3.11	141.72	—	295 ± 4	4.24	142.54	31.7
Methanol	673 ± 183	7.32	138.04	39.4	393 ± 11	10.78	132.18	71.3
Crosslinking	700 ± 224	6.05	90.59	62.2	429 ± 8	8.48	104.53	102.2
Methanol/crosslink	630 ± 179	8.33	102.64	83.1	382 ± 12	12.9	96.3	106.5

final PVA solution contained 13.5 wt% PVA and 0.6 wt% MWNTs. The MWNT content based on PVA is 4.5 wt%.

The electrospinning set-up consists of a plastic syringe with a metal syringe needle (21 gauge), a syringe pump (KD scientific), a high voltage power supply (ES30P, Gamma High Voltage Research) and a metal roller collector. The plastic syringe, needle and the syringe pump were fixed on a movable tackle driven by a motor, forming the moveable nozzle system. In electrospinning, the MWNTs/PVA solution was placed into the syringe and charged with 20 kV electrical voltage via connecting the syringe needle to the power supply. The grounded electrode was connected to the metal roller, 15 cm away from the needle tip. The flow rate of the MWNTs/PVA solution was controlled at 1.0 ml h^{-1}. During the electrospinning process, the nozzle moved to-and-fro along the axis direction of the metal roller at the speed of 20 cm min^{-1}, while the metal roller rotated at a constant speed of 100 rpm. This system was able to produce relatively large (20×30 cm^2) and uniform nanofibre mats. The thickness of the mats was in the range 70–200 μm. The neat PVA nanofibre mat was also electrospun from 13.5 wt% PVA solution under the same operating conditions.

2.3. Post-spinning treatments of the nanofibres

The as-spun PVA fibres were subjected to different post-spinning treatments as follows:

Soaking in methanol [43]: the nanofibre mat was placed in methanol for 24 h and then dried at 50 °C for 24 h.

Crosslinking with glutaric dialdehyde [47]: the nanofibre mat was placed in a glutaric dialdehyde-acetone solution (0.05 wt%, pH = 2–3 adjusted by HCl) for 4 h, and then curled at 150 °C for 10 min.

Methanol treatment followed by crosslinking: the nanofibre mat was first treated by methanol and then crosslinked with glutaric dialdehyde, under the same conditions as above.

3. Results and discussion

3.1. Microscopy observation

Electrospinning the plain PVA solution and the PVA solution containing MWNTs both resulted in uniform nanofibres. The average diameters of the as-spun nanofibres are listed in table 1. For the neat PVA nanofibres, the average fibre diameter was about 680 nm. However, the presence of MWNTs resulted in much finer nanofibres, with an average diameter of 295 nm (table 1), and the fibre distribution became very narrow as well. The large reduction in fibre diameter suggests that the presence of carbon nanotubes in PVA solution affected the fibre stretching process.

The post-spinning treatments only had a marginal effect on both the average diameter and the uniformity of the nanofibres. As listed in table 1, the neat PVA nanofibres treated by methanol showed a small decrease in average fibre diameter, while the crosslinking reaction led to slightly thicker fibres. For the MWNTs/PVA composite nanofibres, both methanol and crosslinking treatments led to a slight increase in average fibre diameter (figure 1).

To examine nanotube dispersion in the PVA matrix, the as-spun nanofibres solidified within a resin were sliced into specimens of 100 nm thick and observed under the TEM. Figure 2 gives a view of the dispersed carbon nanotubes. It also confirmed the existence of carbon nanotubes in the nanofibre mat.

3.2. FTIR spectra

The FTIR spectra of the PVA nanofibres containing MWNTs before and after the crosslinking reaction are shown in figure 3. After the crosslinking reaction, vibration peaks at around 917, 1096 and 1144 cm^{-1} were increased, which correspond to the CH_2 rocking, C–O stretching and C–O–C bending vibration, respectively. The vibration peak in the range of 1235–1340 cm^{-1} was decreased, confirming the reduction of C–H wagging and CH–OH bending vibrations. Also, an increase in the absorbance of 1700 cm^{-1} is attributed to the C=O group of the aldehyde. These changes in the FTIR spectra confirmed the occurrence of a crosslinked network after the nanofibres were treated with glutaric dialdehyde [48–50].

3.3. Differential scanning calorimetry (DSC)

Figure 4(a) shows the DSC profiles measured for the neat PVA nanofibres. All the nanofibres have an endothermic peak around 200–225 °C, corresponding to the melting of PVA (T_m). The T_m values were listed in table 2. The post-treatments shifted the T_m peak. Compared with the untreated nanofibres, methanol treatment shifted T_m to a higher temperature, while the T_m was reduced after the crosslinking reaction.

To compare the crystallinity, enthalpy (ΔH) values were calculated by numerical integration of the area under the melting peak and normalized for sample mass. The increase in crystallinity for the PVA was calculated using the enthalpy of 155 J g^{-1} for a theoretical 100% crystalline PVA [33]. The neat PVA nanofibres have a relatively low crystallinity, at just about 28.8%. The crystallinity of the methanol-treated PVA nanofibres increased to 37.4%, but the crosslinking reaction reduced its crystallinity slightly, due to the change of

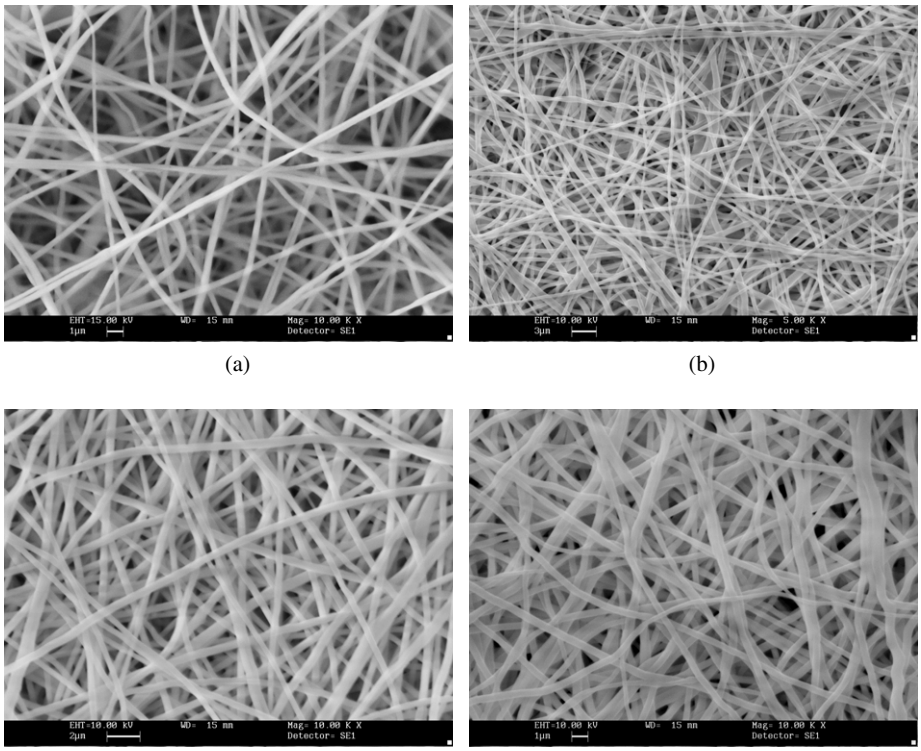

Figure 1. SEM images of the MWNTs/PVA nanofibres, (a) without treatment, (b) treated by methanol, (c) treated by crosslinking, (d) treated by methanol/crosslinking.

Figure 2. TEM image of the MWNTs/PVA nanofibres treated by methanol/crosslinking.

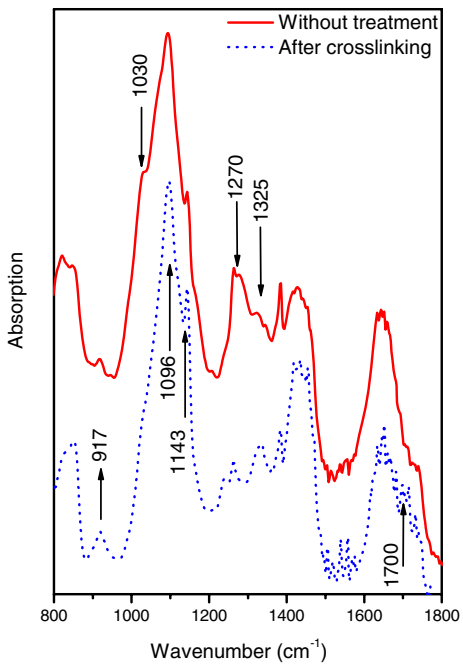

Figure 3. FTIR spectra of the MWNTs/PVA nanofibres before and after crosslinking reaction.

crystalline morphology induced by the crosslinker [51]. The crystallinity of the PVA nanofibres treated by both methanol and the crosslinking reaction is between those treated by the two methods separately.

It is also worth noting that the neat PVA nanofibres contain a certain amount of water as indicated by a peak in the range of 130–170 °C in the DSC curves, though the samples have been dried in vacuum for 72 h before testing. This peak disappeared when the sample was scanned for the second time under the same condition. A similar phenomenon was observed in the MWNTs/PVA film [38]. The post-spinning treatments also

Table 2. Melting point, crystallinity content and thermal degradation data.

	Pure PVA nanofibres						MWNTs/PVA nanofibres					
	T_m (°C)	ΔH (J g^{-1})	χ (%)	Onset (°C)	1st peak	2nd peak	T_m (°C)	ΔH (J g^{-1})	χ (%)	Onset (°C)	1st peak	2nd peak
Non-treatment	218.0	44.6	28.8	215	243	442	221.1	53.2	34.3	201	286	441
Methanol	222.2	57.9	37.4	269	369	575	213.8	61.3	39.5	262	365	442
Crosslinking	211.5	41.8	27.0	245	294	510	217.9	56.1	36.2	258	359	430
Methanol/crosslink	216.8	44.0	28.4	253	310	522	214.1	62.2	40.1	261	357	424

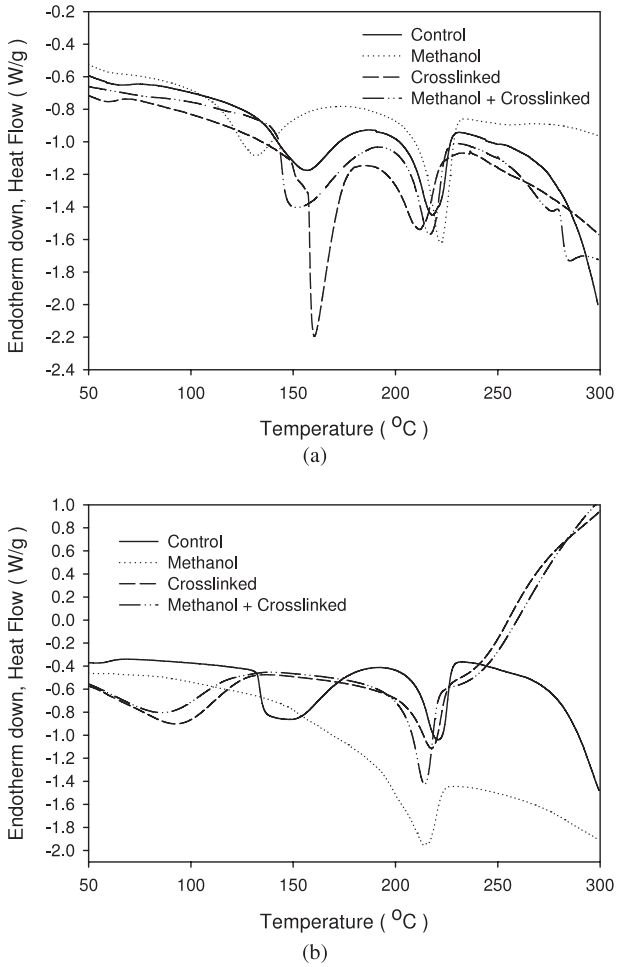

Figure 4. DSC curves of (a) neat PVA nanofibres and (b) MWNTs/PVA (4.5 wt%) nanofibres.

affected both the location and height of this peak, indicating that water molecules in PVA could be incorporated into the amorphous phase. The peak reduced and shifted to a lower temperature as a result of methanol treatment, confirming that the methanol treatment removed some water from the polymer because of the increased PVA crystallization. However, this peak shifted to a higher temperature after the crosslinking reaction, suggesting that the water molecules could be trapped in the crosslinked PVA network.

By contrast, all MWNTs/PVA composite nanofibres showed higher crystallinity. As listed in table 2, the crystallinity of the untreated MWNTs/PVA nanofibres is 34.3%, about 5.5% higher than its neat PVA counterpart. The increase in the crystallinity of PVA due to the presence of carbon nanotubes indicated the occurrence of nucleation PVA crystallization in the electrospun composite nanofibres, which is similar to the case in cast CNTs/PVA film and wet-spun fibres [2, 33, 34, 36, 38]. As the electrospinning process took place very quickly, it is less likely for the PVA molecules to nucleate crystallization around the carbon nanotubes during the electrospinning process. Since the presence of carbon nanotubes in PVA solution also led to a decrease in the fibre diameter, it is possible that this nucleation crystallization or a self-assembly of PVA on the nanotube surface could happen any time as long as the carbon nanotubes are dispersed in PVA solution before electrospinning.

The post-treatments also affected the T_m temperature and the crystallinity of the MWNTs/PVA composite nanofibres (figure 4(b)). The methanol treatment shifted the T_m to a lower value, and also increased the crystallinity content (39.5%), albeit to a lesser extent. The crosslinking reaction led to a slight decrease in T_m value, but a small increase in the crystallinity, which is quite different to the case for the neat PVA nanofibres. This slight increase in the PVA crystallinity after the crosslinking reaction suggested that the presence of carbon nanotubes restricted the reduction of PVA crystallinity induced by the crosslinker. The highest crystallinity content was found in the composite nanofibres treated by both methanol and crosslinking reaction (40.1%). This result confirmed that the presence of carbon nanotubes in the PVA matrix made the PVA perform differently in the post-spinning treatments.

In addition, water was also observed in the composite nanofibres, and the post-spinning treatments affected the water peak. The methanol treatment removed almost all the water from the composite nanofibres because no water peak was observed in the DSC curve. However, the crosslinking reaction only shifted the peak to a lower temperature.

3.4. Wide-angle x-ray diffraction (WAXD)

The WAXD patterns of the neat PVA nanofibres show a strong (101) peak, at about $2\theta = 19.4°$ [52, 53] (figure 5(a)). The post-spinning treatment was observed to change the (101) diffraction intensity. By comparison to the untreated nanofibres, the nanofibres treated by methanol led to stronger (101) reflection and the occurrence of medium intensity (001) and (002) reflections at 16.0° and 32.5°, respectively. However, when the nanofibres were crosslinked, the (101) reflection was lowered considerably. The PVA nanofibres treated by methanol and crosslinking reaction showed a slight reduction in the (101) diffraction intensity.

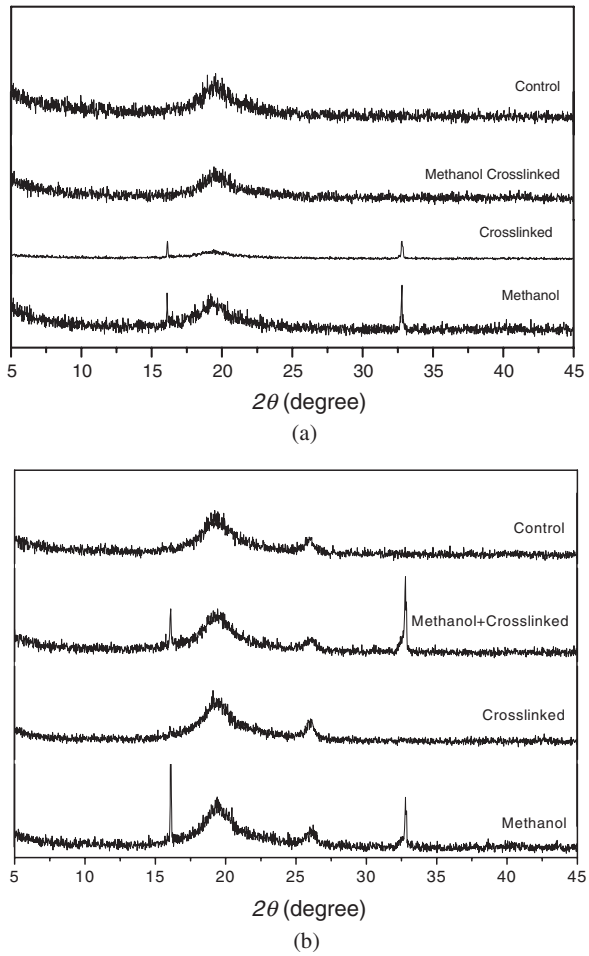

Figure 5. Wide-angle x-ray diffraction: (a) neat PVA nanofibres and (b) MWNTs/PVA nanofibres.

The composite MWNTs/PVA nanofibres not only showed a stronger (101) reflection, but also had a medium intensity (201) peak at $2\theta = 27°$ (figure 5(b)). The post-spinning treatments also influenced the diffraction patterns. Similar to the neat PVA nanofibres, the methanol treatment resulted in a greater (101) peak, and the emergence of (001) and (002) peaks. However, the crosslinking reaction did not reduce the (101) reflection much, which is quite different to the neat PVA nanofibres.

3.5. Mechanical properties

Tensile strength and strain values of both the neat PVA and the MWNTs/PVA composite nanofibre mats are listed in table 1. The tensile strength and strain of the neat PVA nanofibre mat were 7.3 MPa and 141%, respectively. The methanol treatment doubled the tensile strength of the nanofibre mat, but slightly decreased its strain at break. The crosslinking treatment also increased the tensile strength of the nanofibre mat, but resulted in a lower strain value than the methanol treatment.

All composite nanofibres have higher tensile strength than their PVA nanofibre counterparts. Without any post-spinning treatment, the tensile strength of the MWNTs/PVA nanofibre mat was 4.24 MPa, about 36.3% higher than that of the neat PVA counterpart. The post-spinning treatments improved the tensile strength. The methanol treatment led to 2.54 times increase in the tensile strength, and the crosslinking treatment doubled the tensile strength value. The nanofibre mat treated by both methanol and the crosslinking reaction showed the highest improvement in the tensile strength, 12.9 MPa, about 3.04 times higher than the untreated composite nanofibre mat.

The tensile strength of electrospun nanofibre mat is associated with material properties, fibre morphology and web structure. As a result of random fibre collection and electrospinning under the same operating condition, the non-woven nanofibre mats have a similar web structure. To some extent, the tensile strength of the nanofibre mat reflects the strength of the constituent nanofibres. From neat PVA to MWNTs/PVA composite and to the post-treatments by methanol and crosslinking reaction, the material tensile strength was improved by 415% in total.

All the post-spinning treatments decreased the strain value. The crosslinked nanofibre mats had a lower strain value than those treated by methanol, because a crosslinked polymer network typically has greater restriction to mechanical deformation.

3.6. Water contact angle

The water contact angles of the PVA and the composite MWNTs/PVA nanofibre mats were listed in table 1. PVA is hydrophilic in general, and the water droplet was adsorbed by the neat PVA nanofibre mat very quickly. The post-spinning treatments led to an increase in water contact angle. By comparison to untreated nanofibre mat, the nanofibre mat treated by methanol had 40° higher contact angle, while the crosslinked nanofibre mat had higher contact angle value than that treated by methanol, because the–OH groups in PVA are converted to acetal groups or ether linkages after crosslinking with glutaric dialdehyde [50].

The composite MWNTs/PVA nanofibre mat had about 30° higher contact angle than the neat PVA nanofibres, and the post-spinning treatments resulted in further increase in the contact angle value. The lowered surface hydrophility resulting from the presence of carbon nanotubes in the PVA matrix suggested that the nucleation crystallization could influence the surface PVA morphology of the composite nanofibres.

As with the electrospinning of a polymer solution containing nanosized fillers, the nanofillers are normally restricted within the inner side of the electrospun nanofibres, leaving a plain polymer shell on the surface [14, 15, 21, 22, 54]. The difference in the contact angle between the neat PVA and the MWNTs/PVA composite nanofibre mats should come from the effect of the carbon nanotube on the PVA crystallinity and fibre surface morphology. Figure 6 shows the correlation between the water contact angle and the crystallinity of PVA. Ignoring the presence of carbon nanotube and methanol treatment, a linear dependence between the PVA crystallinity and the water contact angle was obtained for the non-crosslinked nanofibre samples. It indicated that a higher PVA crystallinity resulted in higher contact angle value. This can be attributed to the fact that the PVA in crystal is more difficult to be dissolved in water than its amorphous state because of stronger intermolecular hydrogen bonds among the PVA

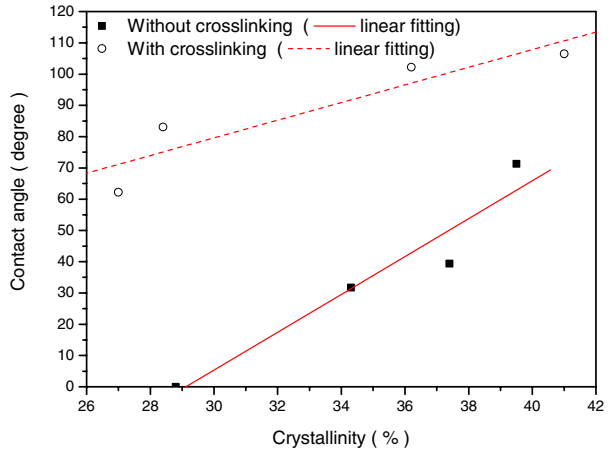

Figure 6. Water contact angle versus crystallinity. The linear fitting for the non-crosslinked nanofibre samples is $\alpha = -176.3 + 6.1\chi$ (correlation coefficient, $R = 0.96$), while for the crosslinked nanofibre samples it is $\alpha = -5.0 + 2.8\chi\,(R = 0.92)$.

molecules in the crystal state [52]. A linear dependence between the PVA crystallinity and the water contact angle was also found for the crosslinked nanofibres, except that the crosslinked nanofibres showed a higher contact angle value.

It was also noticed that the crosslinked composite MWNTs/PVA nanofibres showed a higher contact angle than the untreated one, even if they had similar PVA crystallinity content. This indicated that the crosslinking reaction took place on the surface of the composite nanofibres, but did not change the crystallinity characteristic of the whole nanofibres because of the presence of carbon nanotubes.

3.7. Thermal stability

The thermogravimetric curves give a direct view of polymer thermal degradation. As shown in figure 7(a), the neat PVA nanofibres started to lose weight at about 215 °C, with two main weight loss derivative peaks (DTG) at 243 and 442 °C. The post-spinning treatments increased the onset decomposing temperature (T_d) and shifted the DTG peaks. As listed in table 2, the methanol treatment shifted T_d temperature to 269 °C, about 54 °C higher than that of the untreated PVA nanofibres. Also, the DTG peaks were shifted to a higher temperature. Similar to the methanol treatment, the crosslinking reaction shifted the T_d and DTG peaks to higher temperatures also.

The introduction of MWNTs in PVA resulted in a different thermal degradation process. By comparison with the neat PVA counterpart, the untreated MWNTs/PVA nanofibres have a lower onset decomposing temperature (201 °C), and the second DGA peak was decreased considerably (figure 7(b)). The T_d and DTG peaks of the MWNTs/PVA nanofibres are also listed in table 2. For the untreated composite nanofibres, the first and second DTG peak temperatures were at 286 °C, and 441 °C, respectively. All the post-spinning treatments increased the T_d to about 260 °C, and shifted the first DTG peak to about 360 °C, while the second DTG peak remained almost unchanged. The thermal degradation characteristics among the post-treated MWNTs/PVA nanofibres were quite

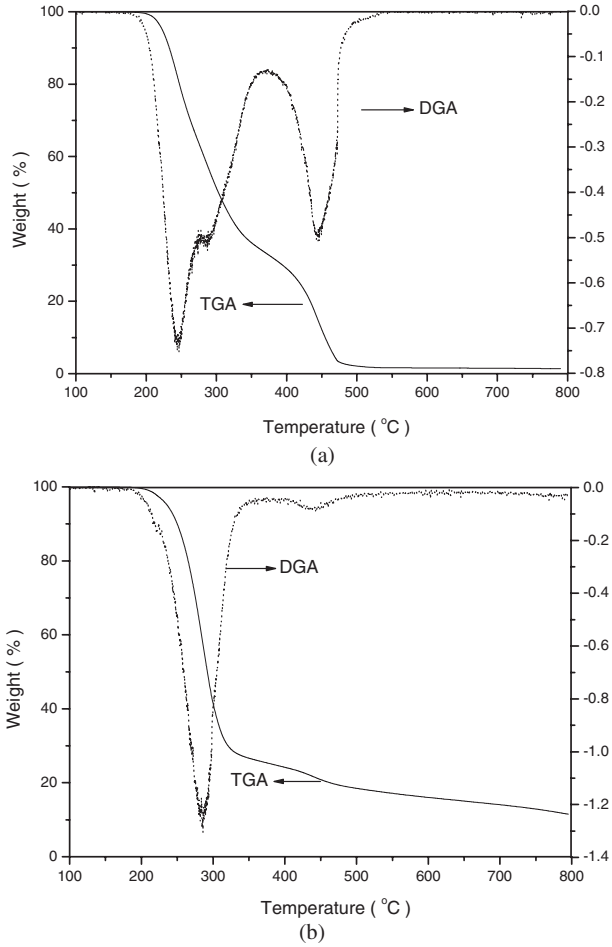

Figure 7. TGA curves of (a) neat PVA nanofibres and (b) MWNTs/PVA nanofibres.

similar to each other. The presence of carbon nanotubes could stabilize the thermal degradation for the post-treated composite nanofibres.

4. Conclusions

This study has confirmed that the nucleation crystallization of PVA by carbon nanotubes also happens in electrospun CNTs/PVA composite nanofibres. This nucleation crystallization process is more likely to take place prior to electrospinning owing to the rapid fibre stretching and the solidification process during electrospinning provides a very limited time for the PVA to crystallize around the carbon nanotube. The increase in the crystallinity due to the presence of carbon nanotubes has considerably improved the tensile strength, but slightly reduced the strain at break of the CNTs/PVA nanofibre mats. The fibre tensile strength can be further improved through increasing the PVA crystallinity or the formation of crosslinked PAV network via soaking in methanol and a crosslink reaction, respectively. However, the presence of carbon nanotubes reduces the crystallization rate in the methanol treatment, but prevents the crystallinity reduction during the crosslinking reaction. With the increase in the PVA crystallinity, fibre tensile strength was further increased, but the

surface hydrophilicity reduced. In comparison to the crosslinking reaction, the methanol treatment resulted in better improvement in the fibre tensile strength and less reduction in the strain value.

These results suggest that the tensile strength and the surface hydrophobicity of CNTs/PVA composite fibres can be improved by a post-spinning treatment to increase the crystallinity of the PVA matrix or by establishing a crosslinked PVA network. A polymer that is able to form nucleation crystallization around carbon nanotubes should be a better choice to develop CNT composite nanofibres because of the enhanced interaction between carbon nanotube and the polymer matrix. Combining the nucleation crystallization of polymer matrix and post-treatments to improve matrix crystallinity will form an effective approach for developing high strength CNT composite materials.

Acknowledgments

This work was carried out through an International Postgraduate Research Scholarship (IPRS) awarded to the first author. The work was also supported by Deakin University under its Central Research Grant scheme.

References

[1] Ajayan P M 1999 *Chem. Rev.* **99** 1787–99
[2] Cadek M, Coleman J N, Barron V, Hedicke K and Blau W J 2002 *Appl. Phys. Lett.* **81** 5123–5
[3] Dalton A B, Collins S, Munoz E, Razal J M, Ebron V H, Ferraris J P, Coleman J N, Kim B G and Baughman R H 2003 *Nature* **423** 703
[4] Kilbride B E, Coleman J N, Fraysse J, Fournet P, Cadek M, Drury A, Hutzler S, Roth S and Blau W J 2002 *J. Appl. Phys.* **92** 4024–30
[5] Sandler J K W, Kirk J E, Kinloch I A, Shaffer M S P and Windle A H 2003 *Polymer* **44** 5893–9
[6] Biercuk M J, Liaguno M C, Radosavljevic M, Hyun J K, Fischer J E and Johnson A T 2002 *Appl. Phys. Lett.* **80** 2767–9
[7] Wei C, Srivastava D and Cho K 2002 *Nano Lett.* **2** 647–50
[8] Vigolo B, Penicaud A, Coulon C, Sauder C, Pailler R, Journet C, Bernier P and Poulin P 2000 *Science* **290** 1331–4
[9] Poulin P, Vigolo B and Launois P 2002 *Carbon* **40** 1741–9
[10] Munoz E *et al* 2004 *Adv. Eng. Mater.* **6** 801–4
[11] Dalton A B, Collins S, Razal J, Munoz E, Ebron V H, Kim B G, Coleman J N, Ferraris J P and Baughman R H 2004 *J. Mater. Chem.* **14** 1–3
[12] Zhang X, Liu T, Sreekumar T V, Kumar S, Hu X and Smith K 2004 *Polymer* **45** 8801–7
[13] Kozlov M E, Capps R C, Sampson W M, Ebron V H, Ferraris J P and Baughman R H 2005 *Adv. Mater.* **17** 614–7
[14] Ko F, Gogotsi Y, Ali A, Naguib N, Ye H, Yang G, Li C and Wilis P 2003 *Adv. Mater.* **15** 1161–5
[15] Dror Y, Salalha W, Khalfin R L, Cohen Y, Yarin A L and Zussman E 2003 *Langmuir* **19** 7012–20
[16] Reneker D H and Chun I 1996 *Nanotechnology* **7** 216–23
[17] Theron S A, Zussman E and Yarin A L 2004 *Polymer* **45** 2017–30
[18] Li D and Xia Y 2004 *Adv. Mater.* **16** 1151–70
[19] Subbiah T, Bhat G S, Tock R W, Parameswaran S and Ramkumar S S 2005 *J. Appl. Polym. Sci.* **96** 557–69
[20] Shin Y M, Hohman M M, Brenner M P and Rutledge G C 2001 *Appl. Phys. Lett.* **78** 1149–51
[21] Gao J, Yu A, Itkis M E, Bekyarova E, Zhao B, Niyogi S and Haddon R C 2004 *J. Am. Chem. Soc.* **126** 16698–9
[22] Salalha W, Dror Y, Khalfin R L, Cohen Y, Yarin A L and Zussman E 2004 *Langmuir* **20** 9852–5
[23] Zhou W, Wu Y, Wei F, Luo G and Qian W 2005 *Polymer* **46** 12689–95
[24] Ge J J, Hou H, Li Q, Graham M J, Greiner A, Reneker D H, Harris F W and Cheng S Z D 2004 *J. Am. Chem. Soc.* **126** 15754–61
[25] Hou H, Ge J J, Zeng J, Li Q, Reneker D H, Greiner A and Cheng S Z D 2005 *Chem. Mater.* **17** 967–73
[26] Kim G M, Michler G H and Poetschke P 2005 *Polymer* **46** 7346–51
[27] Jeong J S, Jeon S Y, Lee T Y, Park J H, Shin J H, Alegaonkar P S, Berdinsky A S and Yoo J B 2006 *Diamond Relat. Mater.* **15** 1839–43
[28] Sundaray B, Subramanian V, Natarajan T S and Krishnamurthy K 2006 *Appl. Phys. Lett.* **88** 143114/1–3
[29] Wang G, Tan Z, Liu X, Chawda S, Koo J-S, Samuilov V and Dudley M 2006 *Nanotechnology* **17** 5829–35
[30] Zhang X, Liu T, Sreekumar T V, Kumar S, Moore V C, Hauge R H and Smalley R E 2003 *Nano Lett.* **3** 1285–8
[31] Cadek M, Coleman J N, Ryan K P, Nicolosi V, Bister G, Fonseca A, Nagy J B, Szostak K, Beguin F and Blau W J 2004 *Nano Lett.* **4** 353–6
[32] Coleman J N, Blau W J, Dalton A B, Munoz E, Collins S, Kim B G, Razal J, Selvidge M, Vieiro G and Baughman R H 2003 *Appl. Phys. Lett.* **82** 1682–4
[33] Probst O, Moore E M, Resasco D E and Grady B P 2004 *Polymer* **45** 4437–43
[34] Chen W, Tao X, Xue P and Cheng X 2005 *Appl. Surf. Sci.* **252** 1404–9
[35] Ryan K P, Cadek M, Drury A, Ruether M, Blau W J and Coleman J N 2005 *Fullerenes, Nanotubes, Carbon Nanostruct.* **13** 431–4
[36] Ciambelli P, Sarno M, Gorrasi G, Sannino D, Tortora M and Vittoria V 2005 *J. Macromol. Sci.* B **44** 779–95
[37] Minus M L, Chae H G and Kumar S 2006 *Polymer* **47** 3705–10
[38] Bin Y, Mine M, Koganemaru A, Jiang X and Matsuo M 2006 *Polymer* **47** 1308–17
[39] Koski A, Yim K and Shivkumar S 2003 *Mater. Lett.* **58** 493–7
[40] Lee J S, Choi K H, Ghim H D, Kim S S, Chun D H, Kim H Y and Lyoo W S 2004 *J. Appl. Polym. Sci.* **93** 1638–46
[41] Zhang C, Yuan X, Wu L, Han Y and Sheng J 2005 *Eur. Polym. J.* **41** 423–32
[42] Son W K, Youk J H, Lee T S and Park W H 2005 *Mater. Lett.* **59** 1571–5
[43] Yao L, Haas T W, Guiseppi-Elie A, Bowlin G L, Simpson D G and Wnek G E 2003 *Chem. Mater.* **15** 1860–4
[44] Lin T, Fang J, Wang H, Cheng T and Wang X 2006 *Nanotechnology* **17** 3718–23
[45] Zeng J, Aigner A, Czubayko F, Kissel T, Wendorff J H and Greiner A 2005 *Biomacromolecules* **6** 1484–8
[46] Taepaiboon P, Rungsardthong U and Supaphol P 2006 *Nanotechnology* **17** 2317–29
[47] Wang X, Chen X, Yoon K, Fang D, Hsiao B S and Chu B 2005 *Environ. Sci. Technol.* **39** 7684–91
[48] Krimm S, Liang C Y and Sutherland G B B M 1956 *J. Polym. Sci.* **22** 227–47
[49] Yeom C-K and Lee K-H 1996 *J. Membrane Sci.* **109** 257–65
[50] Hyder M N, Huang T Y M and Chen P 2006 *J. Membrane Sci.* **283** 281–90
[51] Park J-S, Park J-W and Ruckenstein E 2001 *J. Appl. Polym. Sci.* **82** 1816–23
[52] Assender H E and Windle A H 1998 *Polymer* **39** 4295–302
[53] Nishio Y and Manley R S 1998 *Macromolecules* **21** 1270–7
[54] Liu J, Wang T, Uchida T and Kumar S 2005 *J. Appl. Polym. Sci.* **96** 1992